

# Facile synthetic strategy for efficient and multi-color fluorescent BCNO nanocrystals

Xiaofeng Liu,<sup>\*a,b</sup> Song Ye,<sup>c</sup> Yanbo Qiao,<sup>a,b</sup> Guoping Dong,<sup>a,b</sup> Qiang Zhang,<sup>a,b</sup> and Jianrong Qiu<sup>\*,c</sup>

<sup>a</sup> State Key Laboratory of High Field Laser Physics, Shanghai Institute of Optics and Fine Mechanics, Chinese Academy of Sciences, Shanghai 201800, P. R. China,  
E-mail: xfliu@yahoo.cn

<sup>b</sup> Graduate School of the Chinese Academy of Sciences, Beijing 100039, P. R. China

<sup>c</sup> State Key Laboratory of Silicon Materials, Zhejiang University  
Hangzhou, 310027, P. R. China, E-mail: qir@zju.edu.cn

## Electronic Supplementary Information

### 1. Experimental

Reagent grade boric acid ( $H_3BO_3$ ), urea ( $CO(NH_2)_2$ ), and polyethylene glycol (PEG , MW=20000) were used as the sources for boron, nitrogen and carbon, respectively. The modified O'connor's method was used for the synthesis of bulk materials, which is a mixture of  $B_2O_3$  and BCNO compound (structurally the same as turbostratic boron nitride (t-BN)) nanoscale domains. We fixed the atomic ratio of B/C=0.5, and changed the B/N ratio from 0.2 to 0.5, to control the emission spectra of the obtained products. In the first step, the raw materials mixture were heated to 800°C and kept at this temperature for 30 min and then allowed to cool naturally to ambient temperature. The as-synthesized products were then soaked in distilled water to remove the residual  $B_2O_3$ , leaving the nanosized BCNO nanocrystals (NCs) in the solutions. A semi-quantitative elemental analysis by XPS confirmed that the carbon concentration in the NCs increased with the increase of B/N ratio in the starting materials (Table S1). Particles with larger size were removed by centrifugation at 4000 rpm for 10 min. The remained nanosized BCNO particles in the solution were then collected by another centrifugation at 10000 rpm for 20 min. The obtained BCNO NCs were readily re-dispersed in water for optical characterization.

The structural as well as the morphological properties of the products were characterized with X-ray diffraction (XRD, Rigaku, D/MAX-RA), transmission electron microscopy (TEM, JEOL-2010F) and scanning electron microscopy (SEM, JEOL-6360LA). The chemical bonding state was examined with Fourier-transformation infrared (FT-IR) spectroscopy by the Nicolet 7500 instrument using KBr pellets, and X-ray photoelectron spectroscopy (XPS) with a PHI 550 EACA/SAM photoelectron spectrometer using Al Ka (1486.6 eV) radiation. Electron paramagnetic resonance (EPR, Bruker A300 EPR) spectra for the specimen were collected to give a preliminary explanation of the origin of the fluorescence. Fluorescence spectra and absorption spectra were collected with a JASCO FP-6500

spectrofluorometer, and a JASCO V-570 spectrophotometer. A regeneratively amplified femtosecond (fs) laser (800 nm, pulse duration 120 fs) was used as the two-photon excitation source. The photostability of the NC solution under continuous excitation with monochromatic ultraviolet light at 365 nm ( $\sim$ 1.8 mW), and fs laser (20 mW) excitation, were examined using the function of *time course measurement* of the JASCO FP-6500 equipment. Besides, the fluorescence intensity of the colloid after stored for 1 to 7 days after synthesis has also been examined so as to know the long-term degradation behavior of the NCs.

## 2. X-ray diffraction (XRD)

The XRD patterns of as-synthesized product from the urea route with different boron to nitrogen (B/N) ratios are given in Fig. S1. It can be unambiguously identified that the products mainly comprise crystalline and glassy boron oxide, and t-BN. The relative composition of the two phases depends on the ratio of B/N in the starting materials.

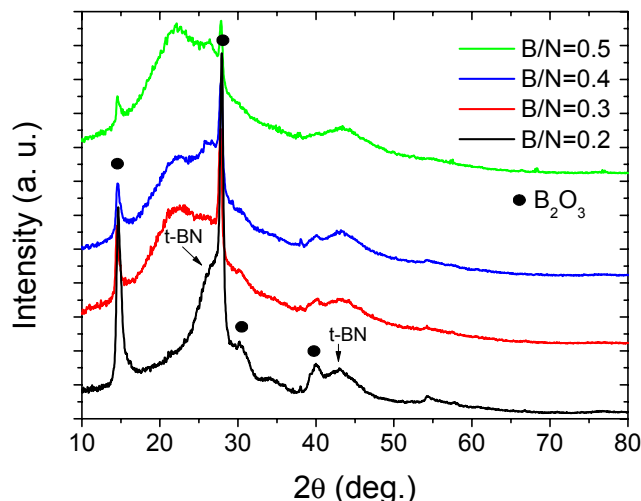


Fig. S1. XRD patterns of as-synthesized products from the urea route with different boron to nitrogen (B/N) ratios. The broad peak centered on  $22^\circ$  is attributed to an amorphous phase, most probably glassy  $\text{B}_2\text{O}_3$ .

## 3. Scanning electron microscopy (SEM)

Morphological observation with SEM for the as-synthesized product from the urea route (before water treatment) is presented in Fig. S2. The products is composed conglomerate large particles of several hundreds microns. No obvious difference can be found between specimens starting from different B/N ratios. The present of B, C, N, and O is confirmed in all the products by energy dispersive spectroscopy (EDS).

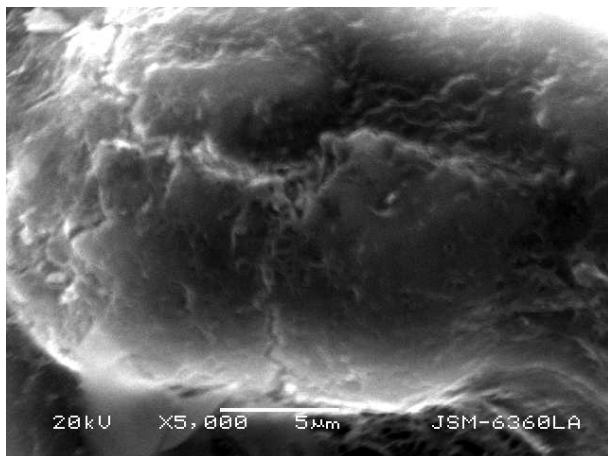


Fig. S2. Representative SEM images of the as-synthesized product (B/N=0.2) from the urea route

#### 4. Fourier transformation infrared (FT-IR) spectroscopy

The strong absorption bands characteristic of t-BN can be found on  $800\text{ cm}^{-1}$  and  $1400\text{ cm}^{-1}$  (Fig. S3), which is attributed to the in-plane and out-of-plane vibration modes of the  $sp^2$  bonded BN.<sup>[1, 2]</sup> Besides, additional bands due to OH and BO groups is also present in the IR spectra.<sup>[2]</sup> Moreover, introduction of the carbon to the system do not result in any observable change in the shape of the IR spectra, indicating that the carbon amount in the as-formed BCNO NCs maybe minimal.

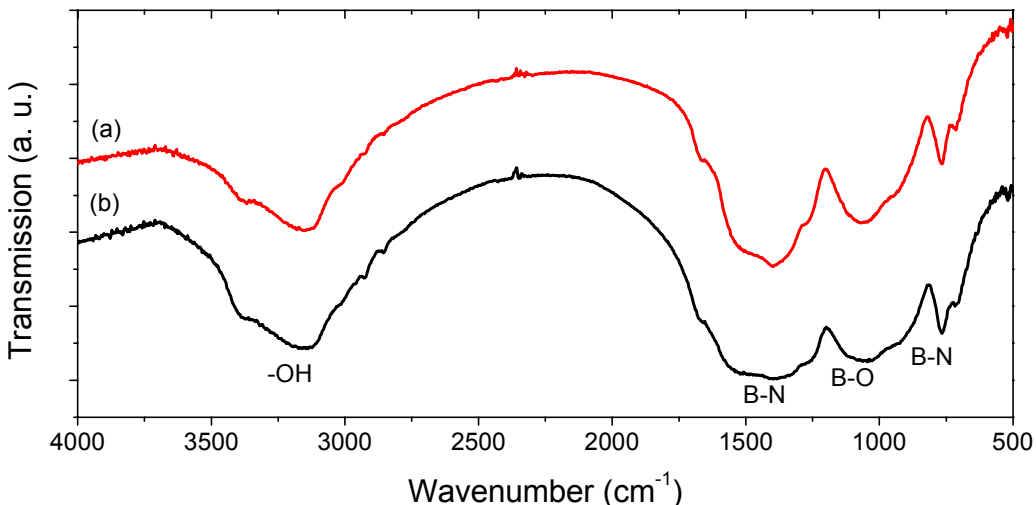


Fig. S3. Infrared spectra of (a) the BCNO NCs (synthesized with B/N=0.2, B/C=0.5), and (b) the sample synthesized without addition of carbon (PEG).

#### 5. X-ray photoelectron spectroscopy (XPS)

The BCNO NCs obtained from water treatment of the products synthesized with the urea route were examined by XPS. The survey-scanned spectra are shown in Fig. S4. The result of semi-quantitative elemental analysis of the BCNO NCs estimated from peak areas corresponding to B, C, N, and O 1s region are given in Table S1. Note that particles surfaces are usually contaminated by organic adsorbents and XPS only gives

information of the samples within limited depth under the surface (<10 nm), the elemental compositions given in Table S1 cannot be recognized as the precise atomic composition for the nanoparticles, especially for C and O. Therefore, these results given by XPS cannot be considered to contradict with the EDS result by transmission electron microscope (TEM), which gives a B/C/N/O of 41/4/46/9.

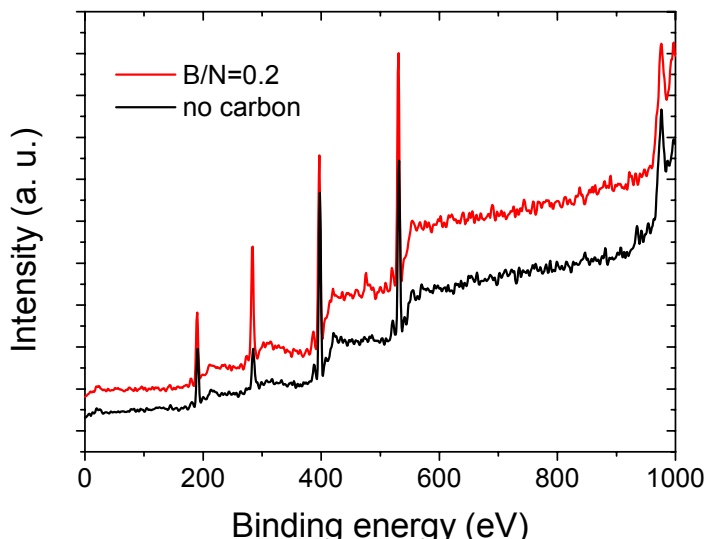


Fig. S4. Survey-scanned XPS spectra of the BCNO NCs ( $B/N=0.2$ ), the sample synthesized without addition of carbon (PEG) is given for a comparison.

Table S1. Semi-quantitative elemental analysis with XPS. (in atom%)

specimens	B	C	N	O
BNO*	36.31	7.64	33.93	22.12
B/N=0.2	34.91	11.60	33.38	20.11
B/N=0.3	30.21	18.57	29.19	22.03
B/N=0.4	27.65	26.77	26.56	19.02
B/N=0.5	27.02	26.90	23.28	22.80

\* BNO denotes the sample synthesized without addition of carbon

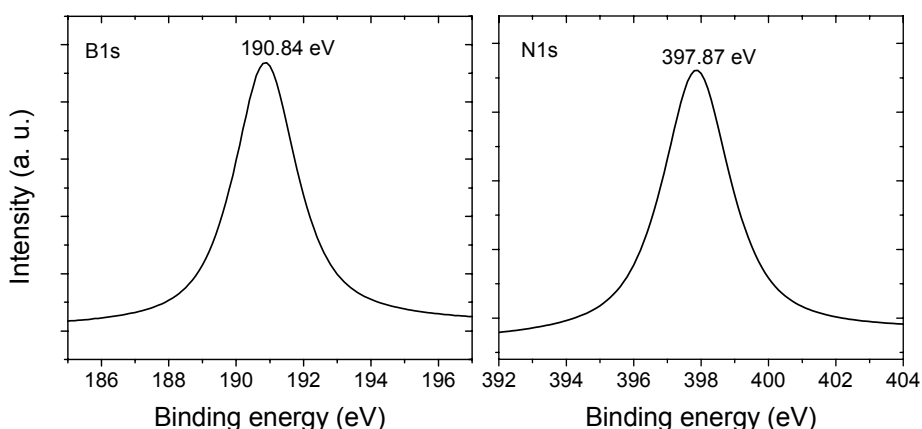


Fig. S5. Fine-scanned XPS spectra in the B1s and N1s region for the BCNO NCs synthesized with  $B/N=0.2$ .

The fine-scanned XPS spectra for all the samples were measured. Fig. S5 shows a typical spectra for the specimen (B/N=0.2) in the B and N 1s region. Since there is no distinct difference in spectral shape, we only summarize the peak positions in the B 1s and N 1s region for different samples (Table S2). Both of the B 1s and the N 1s region display symmetrical peaks located at 190.84 eV and 397.87 eV, respectively, which is the characteristic value for B-N bonding.<sup>[3]</sup> However, neither the bonding of B-C nor N-C is evidenced from these XPS results; all the spectra show a single symmetrical peak. Based on these results, we confirm that the observed carbon by EDS and XPS primarily comes from surface adsorbents and background for TEM (due to carbon coating in the copper grid). The concentration of carbon in the NCs is very small, but it is enough to cause a change in the optical properties of the NCs.

Table S2 Peak positions of in the B and N 1s region for different specimens.

specimens	B 1s (eV)	N 1s (eV)
B/N=0.2	190.84	397.87
B/N=0.3	190.52	397.80
B/N=0.4	190.80	397.83
B/N=0.5	190.33	397.79

## 6. Determination of quantum yield

The quantum yields of the different BCNO NCs aqueous colloid were determined by comparison with ethanol solution of rhodamine B solution (quantum yield: 70%). The quantum yield was calculated using the equation below:<sup>[4]</sup>

$$\eta_s = \eta_r (A_r / A_s)(I_r / I_s)(n_s^2 / n_r^2)(D_s / D_r) \quad (1)$$

$\eta$  is the external quantum yield; A is the absorbance (in  $\text{cm}^{-1}$ ) of the solution or the glass samples; n is the reflective index of the solvent (for water n=1.333, and for ethanol n=1.362); I is the intensity of the excitation light for the reference and samples; and D is the integrated intensity of the emission peaks. The subscripts s and r stand for the measured samples and the standard references. The results are summarized in Table S3.

## 7. Determination of the two-photon action cross section

The two-photon action cross section ( $\varphi_{2P}$ ) is defined as the product of the two-photon absorption cross section and the quantum yield of two-photon induced luminescence, i. e.  $\varphi_{2P} = \eta_{2P} \cdot \sigma_{2P}$ .<sup>[5]</sup> In the present investigation,  $\varphi_{2P}$  for the different BCNO NCs aqueous colloid were roughly estimated by comparing the two-photon induced fluorescence intensity of the colloid samples with that of the reference (rhodamine B solution) under the same experimental conditions using the following equation:<sup>[6]</sup>

$$\varphi_{2P}^s = \varphi_{2P}^r (I^s / I^r) \quad (2)$$

Where  $I$  is the integrated luminescence intensity and the superscripts s and r stand for the measured samples and the standard references.  $\varphi_{2P}^r$ , the two-photon action cross section for rhodamine B, is adopted from Ref. [7]. The obtained results are summarized in Table S3.

Table S3 Calculated quantum yield (QY) and two-photon action cross section for different specimens

specimens	QY (%)	$\varphi_{2P}$ (GM*)
B/N=0.2	9.3	1310
B/N=0.3	20	2360
B/N=0.4	17	2980
B/N=0.5	5.2	570

\* Goeppert-Mayer unit, 1 GM=  $10^{-50}$  cm<sup>4</sup>·s/photon

## 8. Absorption spectra

The absorption spectra of the four different BCNO NCs aqueous colloid are given in Fig. S6. The spectra clearly indicate that the absorption edge shifts towards longer wavelength region with an increase in the B/N ratio during synthesis. This change of absorption is likely caused by the difference in the composition of the products.

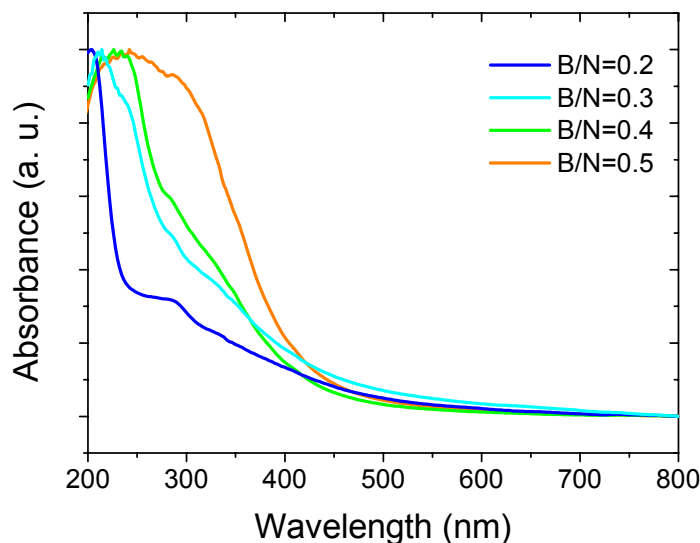


Fig. S6. Absorption spectra of different BCNO NCs aqueous colloid (concentration 0.2wt.%).

## 9. Electron paramagnetic resonance (EPR)

EPR spectra (Fig. S7) confirms the presence a paramagnetic center in the

specimen, with  $g=2.0001$ . Different samples show similar spectral shape and identical  $g$  values. The EPR signal is typical of an electron trapped by defects, probably nitrogen ion vacancy as have previously clarified by other researchers.<sup>[8, 9]</sup> This center is assumed to correlate with the observed colorful emission of BCNO NCs. The detailed mechanisms are going to be discussed in detail in a following investigation.

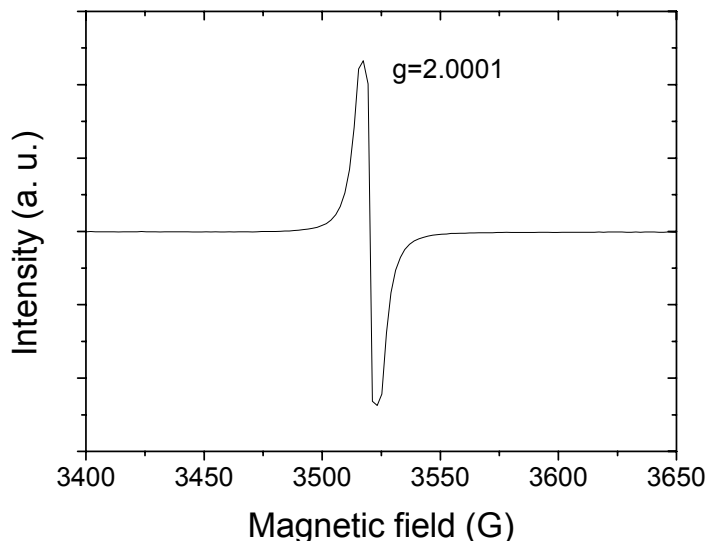


Fig. S7. Typical X-band EPR spectrum of the BCNO NCs (B/N=0.2).

## References

- [1] M. Hubacek, T. Sato, T. Ishii, J. Solid State Chem. 1994, 109, 384.
- [2] V. Brozek, M. Hubacek, J. Solid State Chem. 1992, 100, 120.
- [3] C. D. Wagner, W.W. Riggs, L.E. Davis, J.F. Moulder, G.E. Muilenberg, Handbook of X-ray Photoelectron Spectroscopy, Physical Electronics Division, Perkin-Elmer Corp., Eden Prairie, MN, 1979.
- [4] J. N. Demasa, G. A. Crosby, J. Phys. Chem. 1971, 75, 991
- [5] H. Wang, T. B. Huff, D. A. Zweifel, W. He, P. S. Low, A. Wei, J. Cheng, Proc. Natl. Acad. Sci. U. S. A. 2005, 102, 15752.
- [6] L. Cao, X. Wang, M. J. Meziani, F. Lu, H. Wang, P. Luo, Y. Lin, B. A. Harruff, L. M. Veca, D. Murray, S. Xie, Y. Sun, J. Am. Chem. Soc. 2007, 129, 11318;
- [7] C. Xu, W. W. Webb, J. Opt. Soc. Am. B 1996, 13, 481.
- [8] A. Katzir, J. T. Suss, A. Zunger, A. Halperin, Phys. Rev. B 1975, 11, 2370.
- [9] K. Atobe, M. Honda, M. Ide, H. Yamaji, T. Matsukawa, N. Fukuoka, M. Okada, M. Nakagawa, Jpn. J. Appl. Phys. 1993, 32, 2102.